PERFORMANCE COMPARISON BETWEEN UTRA-TDD HIGH CHIP RATE AND LOW CHIP RATE OPERATION

Ingo Forkel, Xin Jin

Communication Networks (ComNets), Aachen University of Technology, Germany, ingo.forkel@ieee.org

Abstract - The standardization of *UMTS Terrestrial Radio Access* (UTRA) in *Time Division Duplex* (TDD) mode includes two different transmission modes at the physical layer. They differ in their chip rate and with it their bandwidth requirements and characteristics vary. This paper provides a description of the main differences between the *High Chip Rate* (HCR) and *Low Chip Rate* (LCR) options and presents a basic performance comparison of these two modes applied in a micro-cellular urban environment for a single operator in a licensed 3 G band.

I. INTRODUCTION

The wireless communication has seen a rapid development worldwide in recent years. A lot of effort has been spent in worldwide research activities on novel *Time Division Multiple Access* (TDMA) and *Code Division Multiple Access* (CDMA) systems not only in the European RACE[1] and ACTS[2] programs but also in American and Asian countries like the US, China, Korea and especially Japan. Whereas the Japanese and Korean standardization bodies collaborated with the European bodies in relatively early stages of defining third generation *Universal Mobile Telecommunication System* (UMTS), the US focused further on cdma2000 and the Chinese proceed developing the *Time Division Synchronous Code Division Multiple Access* (TD-SCDMA). In 2000, after UMTS Release '99 passed the *3rd Generation Partnership Project* (3GPP) standardization bodies, the Chinese joined the UMTS community and integrated TD-SCDMA into the *UMTS Terrestrial Radio Access* (UTRA) specifications with its own physical layer characteristics [1, 2]. With the introduction of UMTS a new step into future radio communications has been made. Japanese NTDoCoMo launched UMTS in October 2001. The European announce a UMTS startup at the end of 2002. Besides conventional symmetric voice and particular data services, it should also support broadband and asymmetric multimedia services with a wide range of data rates and high *Quality of Service* (QoS).

Two transmission duplex techniques are used in UMTS, *Frequency Division Duplex* (FDD) and *Time Division Duplex* (TDD). Within the TDD operation, two modes are differentiated: TDD *High Chip Rate* (HCR) mode with 3.84 Mcps and TDD *Low Chip Rate* (LCR) mode with 1.28 Mcps. The TDD LCR mode emerged from TD-SCDMA and has become part of UMTS as UTRA TDD LCR from Release 2000 on. The main differences between these two modes are their chip rates, the required bandwidth, the number and structure of time slots used in each radio frame, and the radio frame duration. Furthermore, TDD LCR provides certain synchronization information which caused the "S" in TD-SCDMA.

In this paper, the main focus is to examine the UTRA TDD modes. A performance evaluation of the systems is presented in order to allow a close comparison highlighting the advantages and disadvantages of the two TDD operation modes. By evaluating extensive simulation results the efficiency of UTRA TDD in both modes is confirmed. In the remainder, an introduction into the differences of the two TDD modes is given in Sec. II. Sec. III depicts the scenario and parameters chosen for simulation. The results are summarized in Sec. IV. Finally, some conclusions about the future of UTRA TDD are drawn.

II. CHARACTERISTICS OF HCR AND LCR MODES

In [3], both TDD options are described. The main differences are the chip rates of 3.84 Mcps and 1.28 Mcps and the frame structure. The HCR option uses a radio frame of 10 ms duration divided into 15 time slots each being able to carry a chip sequence of 2560 complex valued chips. At least one slot has to be reserved for *Downlink* (DL) transmission to allow for broadcast information and one for *Uplink* (UL) transmission in order to realize customer's access to the system. The remaining slots can be arbitrarily distributed to either direction in order to adapt to the asymmetry of requested services [4]. Fig. 1 illustrates this structure.

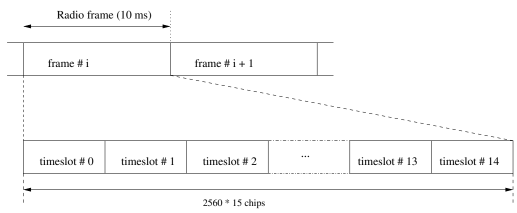

Fig. 1. Radio frame of the 3.84 Mcps TDD option (HCR)

In the LCR option, a 10 ms radio frame is divided into two sub-frames of 5 ms duration. Each of the sub-frames contains seven time slots. Transmission bursts fitting into a single slot contain 864 complex valued chips. The first time slot is always used for DL transmission, the latter six can be divided into UL and DL transmission adaptively, starting with

[1]RACE I & II, Research and Development in Advanced Communication Technologies in Europe, 1989–1995, focused on new cellular concepts with the aim to compare TDMA and CDMA

[2]ACTS, Advanced Communications Technologies and Services, 1994–1998, was a research program with the aim to develop broadband TDMA and CDMA systems as a basis for 3rd generation submissions of ETSI to ITU

the time slots used for UL. Unlike transmission in the HCR mode, the time slots used for LCR transmission in a certain direction have to be grouped together. Between the first two slots in each sub-frame special synchronization and pilot signals are included. The radio frame setup is depicted in Fig. 2.

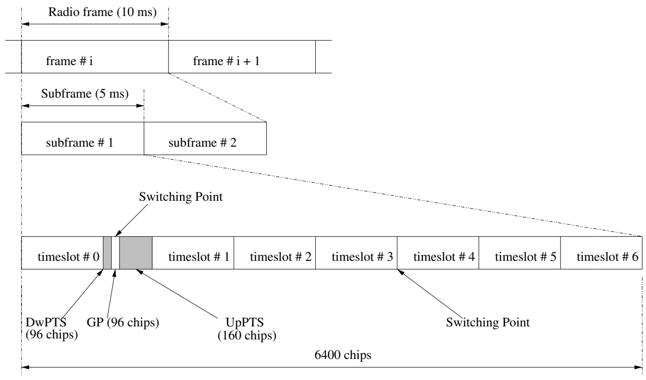

Fig. 2. Radio frame of the 1.28 Mcps TDD option (LCR)

Beneath the information and control data, every burst transmitted in a single time slot contains also a midamble sequence for channel estimation and measurements and a guard period at its end. With burst type 1 in HCR mode, 1952 chips remain for the user and control data. In LCR operation, only 704 chips in each 5 ms sub-frame are available. Hence, a LCR *Resource Unit* (RU) as the combination of spreading code and paired time slots in subsequent sub-frames can only carry about 72% of an HCR RU at the same spreading and modulation layer. Therefore, more RUs may be used to provide the same service in LCR than in HCR.

In order to re-use higher layer protocols, the LCR radio frame is addressed in the same way as the HCR frame, i.e. every 10 ms. Therefore, the information data on *Medium Access Control* (MAC) transport channels—which is almost the same for either mode—has to be distributed to both sub-frames. Hence, the same resources (code and time slot combinations) are used in both of the sub-frames and a frame can be reconfigured earliest after a 10 ms interval.

Another difference is present in the required bandwidth. As Nyquist laws also apply for CDMA technology, the required bandwidth for transmission depends on the fixed chip rate on the physical medium. With only a third of the chip rate, LCR also needs only one third of the spectrum. In the HCR option, one frequency band with a bandwidth of 5 MHz is allocated for an operator, while in the LCR option, there are three frequency bands with a bandwidth of 1.6 MHz each. The carrier distance is thus $1.\bar{6}$ MHz. Fig. 3 illustrates the occupancy of an operator's licensed frequency band with HCR and LCR option.

So unlike HCR operation, *Frequency Division Multiple Access* (FDMA) is used as an additional multiple access technique besides TDMA and CDMA within a single operator's band in the LCR option. The differing arrangements of multiple access techniques in both options result in a differing number of available RU. As a combination of three multiple access techniques by a maximal *Spreading Factor* (SF) of

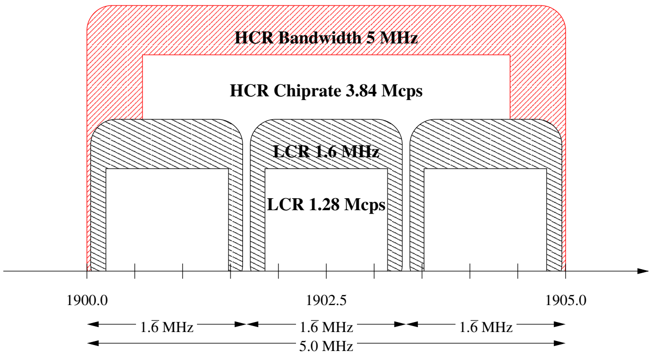

Fig. 3. Spectrum allocation of HCR and LCR frequency bands

16, 240 RU for the HCR and 336 RU for the LCR are calculated as a total for DL and UL transmission. Due to the different bandwidths and the introduction of *Adjacent Carrier Interference* (ACI) in the allocated part of the spectrum, both options are confronted with different interference situations which significantly affect the *Carrier to Interference Ratio* (CIR). The "intra-band" ACI occurring in the LCR mode is illustrated in Fig. 4 where a part of the emitted power is received in the adjacent sub-band due to non-ideal masks and filters at the transmitter and receiver.

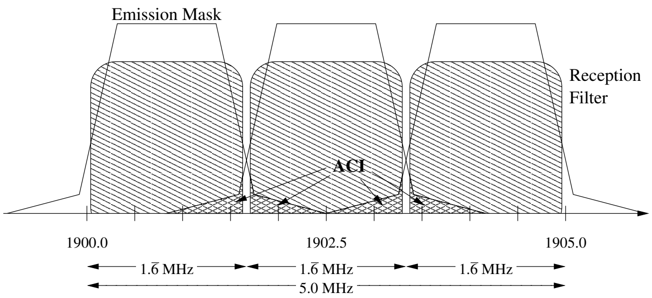

Fig. 4. Adjacent carrier interference in LCR mode due to non-perfect spectral emission masks and reception filters

Dependent on the transmission power P, path loss L, the receiver filter characteristic $H(f)$, and the carrier separation Δf, the ACI I_{adj} can be calculated by

$$I_{adj}(\Delta f, P) = \frac{P}{L} \cdot \int_{-\infty}^{\infty} \Phi(f - \Delta f, P) \cdot |H(f)|^2 df \,. \quad (1)$$

Due to non-linear elements in the transmission amplifier, the spectrum emission mask $\Phi(f, P)$ is dependent on the power P of the transmitter in such a way that the side-band emissions increase faster with increasing power. For a carrier separation of Δf=$1.\bar{6}$ MHz an *Adjacent Channel Interference Ratio* (ACIR) of 43 dB is obtained whereas for the next neighbouring band with separation Δf=$3.\bar{3}$ MHz an ACIR of 54 dB can be calculated. Hence, each transmitted signal will generate additional interference in the neighbouring bands with 43 dB and 54 dB less power, respectively.

III. Simulation Scenario

For simulation purposes, the event-driven and object-oriented simulator GOOSE (Generic Object Oriented Simulation Environment) is used. Fig. 5 depicts the graphical user interface of the tool developed at ComNets. The evaluation is conducted in a Manhattan-like dense urban environment with reference to the simulation guideline in [5]. 60 Node B with omni-directional antennas are located in the streets and placed below rooftop level. Therefore, radio propagation is mainly along the streets (Berg's model [6]) rather than above buildings (Walfish-Ikegami model).

From the 3GPP standard [3] some substantial differences between both options are considered. Tab. 1 summarizes the important parameters used in the simulation.

The differences in the radio frame structure have already been explained in Sec. II. For the *User Equipment* (UE) power, a dynamic range of 80 dB is considered with a maximum of 21 dBm. The Node B total output power is restricted to 43 dBm. Due to joint detection, the dynamic range per time slot is restricted to 3 dB.

Background noise power spectral density N_0 is assumed to be constant within the frequency range of Δf = 5 MHz. For the HCR mode, noise is calculated as

$$N_{\mathrm{HCR}} = N_0 \cdot \Delta f \approx -102\,\mathrm{dBm}.$$

Hence, the background noise power experienced per smaller LCR band is calculated by

$$N_{\mathrm{LCR}} = N_{\mathrm{HCR}} + 10\log(1.6/5) \approx -107\,\mathrm{dBm}.$$

Considering the CIR-based power control, different target levels are chosen for HCR and LCR transmission. This is due to a different mapping of *Adaptive Multi Rate* (AMR) speech service at 7.95 kbps to physical channels. In HCR, 1 code with SF 16 in each link direction is sufficient whereas LCR requires 2 codes with SF 16 in DL and 1 code with SF 8 in UL [7]. With a smaller SF and with this a reduced processing gain, the LCR target CIR has to be at least 3 dB higher. An additional headroom is necessary due to different coding, puncturing, and power control. In DL, the CIR target is set to −9.0 dB in the HCR option and −4.0 dB in the LCR option. In UL, −9.5 dB and −6.0 dB are chosen, respectively.

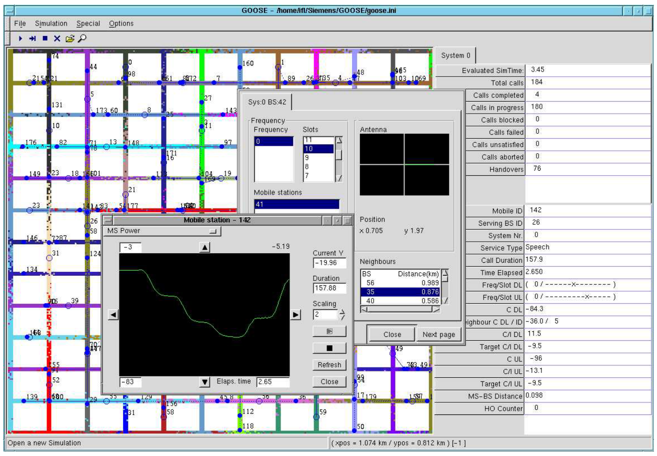

Fig. 5. GOOSE graphical user interface and scenario

Table 1
Simulation parameter

Parameters	HCR	LCR
Chip rate	3.84 Mcps	1.28 Mcps
Frame duration	10 ms	5 ms
Measurement period	10 ms	5 ms
Available frequencies	1	3
DL/UL filter bandwidth	5.0 MHz	1.6 MHz
Frequency range	1900–1905 MHz	
Carrier spacing	5.0 MHz	$1.\bar{6}$ MHz
Time slots (DL/UL)	15 (8/7)	7 (4/3)
UE power range	−59 to +21 dBm	
Node B power	max. +43 dBm	
General noise	−102 dBm	−107 dBm
UL CIR target	−9.5 dB	−6.0 dB
DL CIR target	−9.0 dB	−4.0 dB
Service type	AMR speech at 7.95 kbps	
Service activity	50%	
Spreading factor (DL/UL)	16/16	16/8
Codes needed (DL/UL)	1/1	2/1

IV. Results

Simulation results consider speech as service type with 50% activity and overall traffic from 50 to 90 Erlang per Node B for the two options. In principal, HCR TDD is able to carry up to 112 connections (UL limited by 16 available codes in every of the 7 time slots) and LCR can cope with 72 connections (UL limited by 8 available codes in every of the 3 time slots on every of the 3 frequencies). Therefore, far less traffic is expected in the LCR option.

A main focus of the simulations is the determination and evaluation of the interference situations. Fig. 6 presents the obtained mean interference values with respect to the distance between *Mobile Station* (MS) and its associated Node B or *Base Station* (BS) in the following. The two peaks in the plots reflect two street crossings where high interference due to crossroad traffic is experienced. The background noise of −102 dBm in HCR and −107 dBm in LCR can also be obtained from the curves. The background noise in LCR is 5 dB lower than in HCR, since the bandwidth of a LCR frequency channel is about one third of a HCR channel. On the other hand, the LCR option causes a higher *Noise Rise* (which means an increase in interference above background noise) than the HCR option. This is a result of the higher required target CIR levels in LCR as compared to the HCR system. Furthermore, each LCR frequency channel is influenced by ACI of at least one or even two neighbouring channels. ACI strongly depends on the traffic in the whole system, the more traffic is offered the higher the ACI and the stronger the feedback due to power control reactions will be. On the whole, the interference situation of LCR is better than HCR for low load situations. Anyway, LCR will carry far less traffic than HCR due to the restricted number of available codes. Hence, interference will not be the limiting factor for this network.

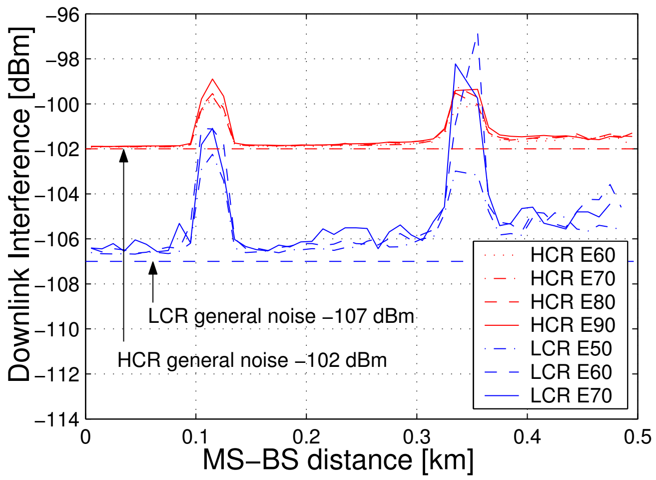

Fig. 6. Distribution of mean interference versus distance in DL

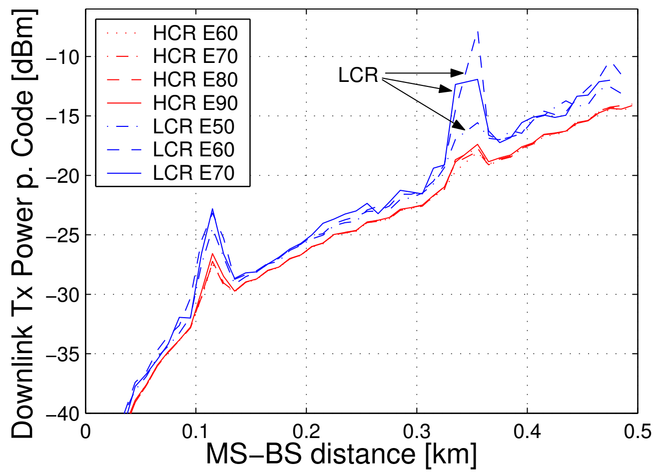

Fig. 7. Distribution of mean transmission power versus distance in DL

The two peaks in Fig. 6 can be found again at corresponding locations in Fig. 7 where the obtained mean BS transmission power values versus distance between MS and BS are presented. To achieve the CIR targets, power control is used to counterbalance the interference time-variantly. A raise in interference on a crossing should be compensated with a higher transmission power. The peak values at a distance of 115 m are noticeable, as they are about 3 dB for HCR and 4 dB for LCR above average at this position. With increasing distance between BS and MS the necessary transmission power increases in order to compensate the growing path loss. Since the noise rise for LCR at the next intersection at 345 m is about 6 dB higher than the normal interference floor (see Fig. 6), the transmission power is also increased by 5–6 dB in this region. However, the total transmission power is sufficient to compensate the interference and not jet restricted by its upper boundary of 43 dBm.

In Fig. 8, the probability distributions of CIR are depicted. Due to the power control inaccuracy caused by a fixed step width Δ_{TPC} of 1 dB, the values are distributed in an intervall of ± 1 dB around the target. In some cases, even the CIR 1 dB below the target are undershot in both options. The probability of CIR values not reaching -10.0 dB is still about 5% for both options. These 5% are caused by time-variant factors like fading, shadowing, and unpredictable changes in the interference situation. An ideal run of the curve would be a straight line from 1 dB below the target with probability 0% to 1 dB above the target with probability 100%. However, the transmission power dynamic range limitations at the BS of 30 dB lead to even higher CIR values for some of the measurements.

This phenomenon can be explained by investigating the CIR values with respect to the link distance in Fig. 9. For close distance to the BS, the measured average CIR are too high because the BS can not further reduce the power. Nevertheless, the CIR values still stay above the required targets of -9.0 dB in HCR option and -4.0 dB in LCR option.

Fig. 11 illustrates the UL mean CIR values with respect to the distance between MS and BS. For a couple of MS closer than 42 m to the Node B, the CIR values increase. These MSs have reached their minimum transmission power and cannot further reduce it as the power control would require.

Fig. 10 illustrates the *Satisfied User Criterion* (SUC) [5] versus the offered traffic in Erlang. The degradation of the SUC is caused by blocked connections. The analytically derived Erlang blocking probability curves for restrictions due to 112 connections for HCR and 72 connections for LCR are plotted additionally. With a lower number of available RU LCR cannot provide as much traffic as HCR. 70 Erlang already cause a SUC of less than 96%. Hence, the main limitation is not the interference but the restricted number of RU.

V. Conclusion

This paper gives a basic comparison of the two UTRA TDD operation modes with 3.84 Mcps and 1.28 Mcps, i.e. the HCR and LCR option. Differences of the physical layer characteristics are described and the performance of these networks is evaluated by means of dynamic simulation.

Simulation results show that the LCR mode offers better connection quality in terms of total interference but higher noise rise for low load conditions due to a lower background noise floor. With increasing number of UE to be served, interference is getting worse in both operation modes. But with the higher power control target levels necessary for the LCR system it seems to loose its advantage over HCR for higher traffics.

However, the main limitation in both networks concerning speech service is not the interference but the restricted number of radio resources. Especially the LCR system suffers from these restrictions and can only provide up to 65 speech connections per BS in parallel whereas HCR can further drive up to 90 Erlang of traffic.

Acknowledgement

The authors would like to thank Prof. B. Walke and R. Pabst of ComNets for their support and advice to this work.

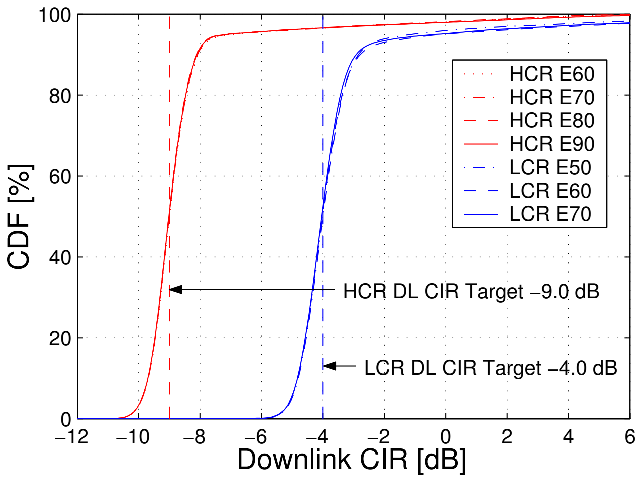

Fig. 8. Distribution of CIR in DL

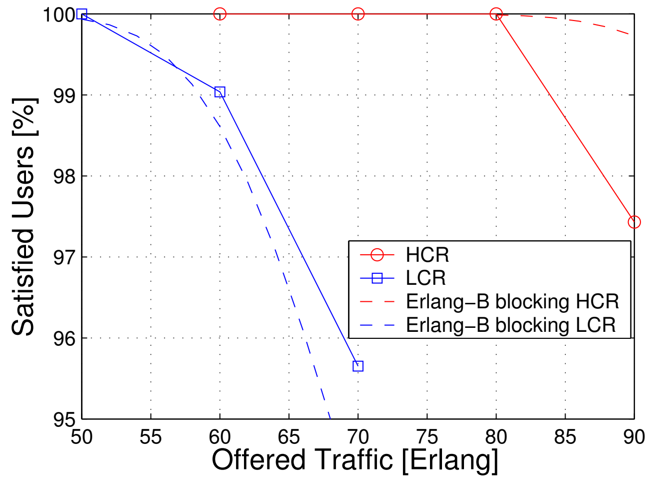

Fig. 10. Satisfied user statistics

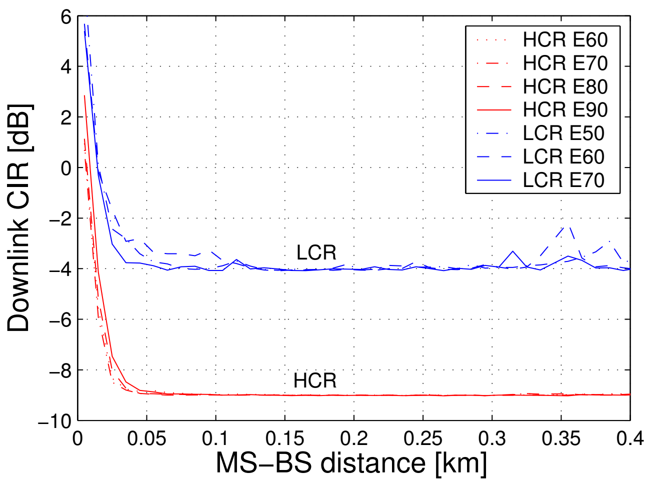

Fig. 9. Distribution of mean CIR versus distance in DL

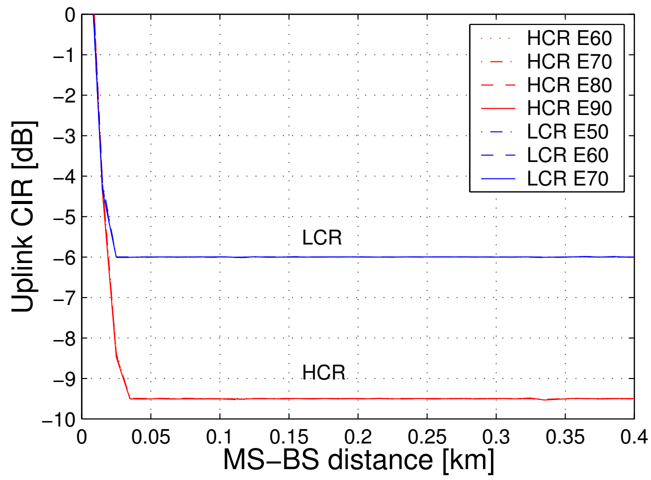

Fig. 11. Distribution of mean CIR versus distance in UL

The friendly input of Siemens, Germany is appreciated.

References

[1] B. Walke, *Mobile Radio Networks*, John Wiley & Sons, Chichester, UK, 2001.

[2] I. Forkel, B. Wegmann, and E. Schulz, "On the Capacity of a UTRA-TDD Network with Multiple Services," in *Proc. ICC 2002*, New York, US, May 2002.

[3] 3GPP, "Physical Channels and Mapping of Transport Channels onto Physical Channels (TDD) (TS 25.221 V 4.1.0 Release 1999)," Tech. Rep., 3rd Generation Partnership Project, June 2001.

[4] W.S. Jeon and D.G. Jeong, "Comparison of Time Slot Allocation Strategies for CDMA/TDD Systems," *IEEE Journal on Selected Areas in Communications*, vol. 18, no. 7, pp. 1271–1278, Aug. 2000.

[5] ETSI, "Selection Procedures for the Choice of Radio Transmission Technologies of the UMTS (UMTS 30.03) (TR 101 112 V 3.2.0)," Tech. Rep., European Telecommunications Standards Institute, Apr. 1998.

[6] J.E. Berg, "A Recursive Method For Street Micro-cell Path Loss Calculations," in *Proc. PIMRC 1995*, 1995, vol. 1, pp. 140–143.

[7] 3GPP, "Universal Mobile Telecommunications System (UMTS); Common Test Environments for User Equipment (UE) Conformance Testing (TS 34.108 V 4.0.0 Release 1999)," Tech. Rep., 3rd Generation Partnership Project, Sep. 2001.